Lateral flow assay-based bacterial detection using engineered cell wall binding domains of a phage endolysin

Minsuk Kong[a,1], Joong Ho Shin[b,1], Sunggi Heu[c], Je-Kyun Park[b,*], Sangryeol Ryu[a,*]

[a] Department of Food and Animal Biotechnology, Department of Agricultural Biotechnology, Center for Food and Bioconvergence, Research Institute of Agriculture and Life Sciences, Seoul National University, 1 Gwanak-ro, Gwanak-gu, Seoul 08826, Republic of Korea
[b] Department of Bio and Brain Engineering, Korea Advanced Institute of Science and Technology (KAIST), 291 Daehak-ro, Yuseong-gu, Daejeon 34141, Republic of Korea
[c] Crop Cultivation and Environment Research Division, National Institute of Crop Science, RDA, Suwon 16429, Republic of Korea

ARTICLE INFO

ABSTRACT

The development of a cost-effective and efficient bacterial detection assay is essential for diagnostic fields, particularly in resource-poor settings. Although antibodies have been widely used for bacterial capture, the production of soluble antibodies is still expensive and time-consuming. Here, we developed a nitrocellulose-based lateral flow assay using cell wall binding domains (CBDs) from phage as a recognition element and colloidal gold nanoparticles as a colorimetric signal for the detection of a model pathogenic bacterium, *Bacillus cereus (B. cereus)*. To improve conjugation efficiency and detection sensitivity, cysteine-glutathione-S-transferase-tagged CBDs and maltose-binding protein-tagged CBDs were produced in *Escherichia coli (E. coli)* and incorporated in our assays. The sensitivity of the strip to detect *B. cereus* was 1×10^4 CFU/mL and the overall assay time was 20 min. The assay showed superior results compared to the antibody-based approach, and did not show any significant cross-reactivity. This proof of concept study indicates that the lateral flow assay using engineered CBDs hold considerable promise as simple, rapid, and cost-effective biosensors for whole cell detection.

1. Introduction

Lateral flow assays (LFAs) are widely used as a rapid detection method for various monitoring and diagnostic purposes. LFAs are particularly useful for on-site use in resource-poor settings because they are easy to use and portable, their results can be interpreted without external equipment, and are usually obtained within tens of minutes (Posthuma-Trumpie et al., 2009). Most LFAs employ several types of antibodies (monoclonal, polyclonal, HRP-conjugated, AP-conjugated, etc.) to capture the analytes and produce detection signals. However, the production of these antibodies requires immunized animals and mammalian cell expression systems, which greatly increases the cost of the diagnostic assays. Despite the ongoing efforts to produce recombinant antibodies in microbial organisms, they are still associated with several problems, including inclusion body formation, inefficient secretion, and lack of post-translational modifications (Frenzel et al., 2013; Robinson et al., 2015; Spadiut et al., 2014). Moreover, there is an increasing concern about the specificity, sensitivity, and stability of these antibodies (Baker, 2015). The use of high-affinity aptamers could be another method to replace expensive antibodies in diagnostics (Chen and Yang, 2015), but the immobilization of small aptamers onto nitrocellulose or other analytical membranes often requires ultraviolet light, which could induce structural changes to the aptamers through thymine dimerization (Bruno, 2014; Smiley et al., 2013). For these reasons, the development of alternative receptor molecules in LFAs to reduce assay cost and provide reliable data has been a topic of great commercial and academic interest.

Bacteriophages produce highly evolved lytic enzymes called endolysins, which help release phage progeny. These endolysins usually have a modular structure consisting of one or several catalytic domains that break down the bacterial cell wall, in addition to a cell wall binding domain (CBD) that recognizes a highly specific ligand in the cell wall and targets the endolysin to its substrate (Schmelcher et al., 2012). Since CBDs have strong affinity and high specificity toward target bacteria and can be easily produced by *E. coli* expression system (Table S1), several groups have tested their potential as a biosensing tool. Walcher et al. combined CBD-based magnetic separation with real-time polymerase chain reaction (PCR) for the detection of *Listeria* cells

in raw milk (Walcher et al., 2010). Tolba et al. immobilized CBDs from *Listeria* phage endolysins on a gold electrode, allowing bacterial detection by electrochemical impedance spectroscopy (EIS) (Tolba et al., 2012). Kong et al. reported a surface plasmon resonance (SPR)-based detection method using *Bacillus cereus* phage CBDs (Kong et al., 2015). In a recent study, Yu et al. used immunomagnetic separation and streptavidin–horseradish peroxidase (strep–HRP) labeled CBDs to detect *Staphylococcus aureus* cells (Yu et al., 2016). Although these CBD-based detection methods presented promising results with a detection limit ranged from 10^2 to 10^5 CFU/mL, sophisticated equipment (PCR, EIS, SPR, etc.) is often required to detect their signals and expensive enzymes/substrates (strep–HRP, 3,3′,5,5′-tetramethylbenzidine) are needed for the assays, hindering the production of low-cost devices.

Here we describe an engineered CBD-based lateral flow assay for the detection of *Bacillus cereus* (*B. cereus*). We chose *B. cereus* as a model organism because *B. cereus* is widely distributed in nature and is an important food pathogen that causes emetic and diarrheal syndromes (Bottone, 2010). The use of engineered CBDs allowed for simple immobilization onto gold nanoparticles and improved detection sensitivity. To the best of our knowledge, this is the first report to describe the use of an engineered CBD in a lateral flow assay format. In addition, this approach does not require primary antibodies or expensive enzyme-conjugated secondary antibodies, enabling the assay to be developed at low cost. This work can thus provide the basis for the development of rapid, cost-effective, and eco-friendly point-of-care diagnostic devices for bacterial detection.

2. Materials and methods

2.1. Materials

Nitrocellulose (NC) strips (15 µm pore size) were purchased from Advanced Microdevices (CNPC-SS12; Ambala Cantt, India) and absorbent pads were purchased from Ahlstrom (Grade 222; Helsinki, Finland). 20 nm gold nanoparticles (AuNPs) suspended in 0.1 mM phosphate-buffered saline (PBS) and AuNPs suspended in citrate buffer were purchased from Sigma-Aldrich (753610, 741965; St. Louis, MO, USA). Methoxypoly(ethylene glycol) functionalized with a thiol group (mPEG-SH, MW: 5000) was purchased from SunBio (Anyang, Korea). To prepare sample solutions containing target bacteria at known concentrations, each bacterial colony was inoculated into tryptic soy broth (TSB), which was purchased from BD Difco (211825; Sparks, MD, USA), and grown overnight. Next, 50 µL of the bacterial culture was diluted with fresh TSB solution (1/100 dilution) and grown until it reached the desired concentration.

2.2. Construction of plasmids

The gene fragment encoding the putative CBD was amplified from LysB4 (Son et al., 2012), digested with *BamHI* and *HindIII* (Takara Clontech, Kyoto, Japan), and ligated into pET28a (Novagen, Madison, WI, USA). For enhanced green fluorescent protein (EGFP)-fused CBD proteins, the *BamHI/HindIII*-digested CBD gene was subcloned into pET28a:EGFP (Kong et al., 2015). For mCherry tagging, the sequence encoding mCherry was subcloned from pmCherry-N1 (Clontech) into pET28a using the *NdeI* and *BamHI* sites. For Cys-glutathione-S-transferase (Cys-GST) tagging, the sequence encoding GST was amplified by PCR using primers that introduced an additional N-terminal single cysteine residue and C-terminal GSGSGS-linker residues. The amplified DNA product was double-digested using *NdeI* and *BamHI* and ligated into the pET28a vector. For maltose binding protein (MBP) tagging, the sequence encoding MBP was amplified using pMBP Parallel 1 as a template (Sheffield et al., 1999), digested with *NdeI*/ *BamHI* (Takara Clontech), and subcloned into 10His-pET28a (Kong and Ryu, 2016). The native stop codons of EGFP, mCherry, GST, and

MBP were omitted for translational fusions. The *BamHI/HindIII*-digested CBD gene was subcloned into the corresponding recombinant plasmids. DNA sequences were verified for all constructs. All constructs had an N-terminal His tag for protein purification. All primers and recombinant plasmids used in this study are listed in Table S2.

2.3. Engineered CBD production

The recombinant CBDs were expressed in *E. coli* BL21 (DE3) cells (Invitrogen, Carlsbad, CA, USA) grown at 37 °C in LB broth supplemented with kanamycin (50 µg/mL). When the optical density of the medium reached approximately 0.8, protein expression was induced using 0.5 mM isopropyl β-D-1-thiogalactopyranoside (IPTG), after which the cultures were incubated overnight at 18 °C. The cells were disrupted by sonication and the CBDs were purified by nickel affinity chromatography using Ni-NTA Superflow resin (Qiagen, Hilden, Germany) as described previously (Kong et al., 2015). For Cys-GST tagged CBD proteins, all purification buffers included 6.25 mM β-mercaptoethanol to maintain a reducing environment. The purified proteins were subjected to gel filtration chromatography through a Sephadex G-25 column (PD MidiTrap G-25; GE Healthcare, Buckinghamshire, UK) with PBS buffer. The final concentrations of the recombinant CBDs were determined by the Bradford assay.

### 2.4. Characterization of the CBD proteins

The binding properties of the EGFP-CBD fusion protein were examined as previously described (Loessner et al., 2002). Briefly, exponentially growing bacterial cells were transferred to Dulbecco's phosphate-buffered saline (DPBS, GenDepot, Barker, TX, USA) and incubated with 0.4 µM EGFP-CBD fusion protein for 5 min at room temperature. The cells were then washed twice with DPBS buffer and observed by epifluorescence microscopy (DE/Axio Imager A1 microscope; Carl Zeiss, Oberkochen, Germany) with a filter set for EGFP (excitation 470/40; emission 525/50). Since mCherry is more tolerant to pH changes than GFP (Doherty et al., 2010), mCherry-tagged CBD proteins were used to examine the effect of NaCl and pH on CBD binding. Quantitative fluorescence assays were conducted using a SpectraMax i3 multimode microplate reader (Molecular Devices, Sunnyvale, CA, USA) with excitation at 485 nm and emission at 535 nm. All quantitative assays were carried out in triplicate.

2.5. Conjugation of gold nanoparticles to CBDs

For CBD conjugation, 10 µL of Tris-Cl (pH 9.0) was added to 1 mL of citrate-stabilized gold nanoparticles (20 nm, Sigma). Then, 15 µg of Cys-GST-tagged CBD proteins was adsorbed at room temperature for 1 h on a rotator. To block and stabilize the CBD-conjugated AuNPs, 100 µL of 2 mM thiol-terminated PEG (5 kDa, dissolved in 10 mM Tris-Cl, pH 9.0) was added to 1 mL of conjugate solution and further incubated for 1 h. Unbound proteins and PEGs were removed by centrifugation (8000×*g*, 4 °C) for 30 min. The final conjugate was resuspended in 1 mL of storage buffer (PBS, pH 7.4, 0.02% bovine serum albumin (BSA)) and stored in a dark bottle at 4 °C.

2.6. Conjugation of gold nanoparticles to antibodies

To test the detection capability of the antibody, we used commercially available anti-*B. cereus* antibody (ab20556; Abcam, Cambridge, UK). For antibody conjugation, 12 µL of K_2CO_3 (0.2 M) was added to 600 µL of AuNP (20 nm, suspended in 0.1 mM PBS) solution to adjust the pH to 9.0. Then, 4 µg of the appropriate antibody was added to the solution, after which the mixture was incubated at room temperature for 20 min. To block nonspecific binding sites on the surfaces of the antibody-conjugated AuNPs, 100 µL of PBS containing 3% BSA was added, after which the mixture was incubated for 20 min. To remove
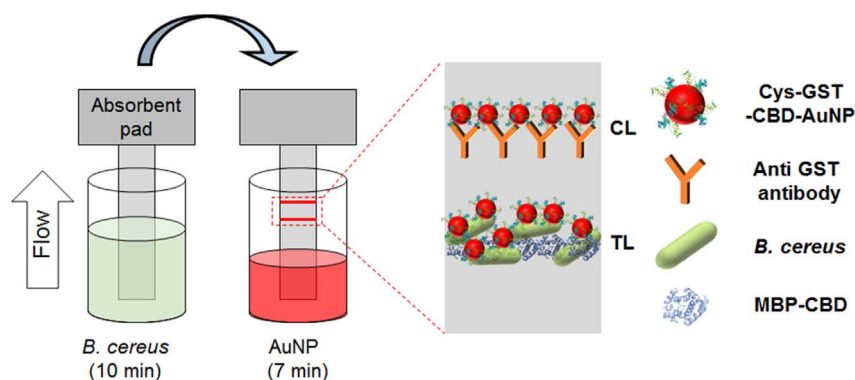
Scheme 1. Schematic diagram of bacteria detection. The strip is sequentially dipped into solutions that contain bacteria and AuNPs for 10 min and 7 min, respectively. The CBD is immobilized on the NC strip as the test line (TL) and the anti-GST antibody is immobilized as the control line (CL) (figure not drawn to scale).

unbound antibodies, the AuNPs were spun by centrifugation at 7000g for 30 min. The supernatant was removed and the AuNPs were resuspended in PBS containing 3% BSA and 0.05% Tween-20.

2.7. Preparation of LFA strips

The purified proteins were dispensed on NC membrane using a commercial dispenser (LPM-02; Advanced Microdevices), after which the membrane was cut into strips 4 mm wide and 25 mm long. The antibody was diluted with PBS and dispensed at 1 mg/mL as a test line. As a control line, 1 mg/mL anti-rabbit IgG-heavy and light chain antibody (120-100A; Bethyl, Montgomery, TX, USA) was dispensed (Scheme 1). To compare the detection capabilities of B4_CBD and MBP-tagged B4_CBD, purified B4_CBD was diluted with PBS containing 5% BSA and dispensed at 0.75 mg/mL; purified MBP-tagged B4_CBD was dispensed at 3.0 mg/mL (also diluted with PBS containing 5% BSA). Anti-GST antibody (A190-122A; Bethyl) was dispensed at 1 mg/mL as a control line. CBDs were diluted with PBS containing 5% BSA in order to minimize the nonspecific signal and increase the detection signal-to-noise ratio (Preechakasedkit et al., 2012).

2.8. Detection of bacteria using the CBD-based paper strip

Optimization studies showed that PBS with 2% BSA was the most appropriate running buffer. *B. cereus* cells were suspended in running buffer and 150 μL was loaded into the wells of a 96-well plate. One end of the strip was dipped into a well, while the other end was attached to two absorbent pads (8×18 mm) to maintain sample flow. After 10 min, the strip was taken out of the well, a new absorbent pad was attached, and the strip was dipped for 7 min into another well that contained 50 μL of AuNP solution (AuNPs were functionalized with either GST-CBD or the commercial antibody). Pictures were taken after the strips were dried.

2.9. ImageJ analysis

The test line area was quantified using ImageJ software (NIH). To this end, a rectangular region of interest was selected containing the test line. The region was then inverted, converted into a 32-bit image, and its average grey scale intensity was measured. Another rectangular region of interest was selected from the background and the aforementioned process was repeated to measure the background intensity. The background intensity value was subtracted from the test line's intensity value to obtain the normalized test line intensity. The limit of detection (LOD) was calculated as the sum of the signal intensity of the 0 CFU/mL reaction and three times its standard deviation (Wang et al., 2015).

3. Results and discussion

3.1. Identification and characterization of a B. cereus-specific B4_CBD

LysB4, an endolysin of *B. cereus* phage B4, is an antibacterial agent that can potentially be used to control foodborne pathogens because it shows strong lytic activity against a broad range of bacteria (Son et al., 2012). LysB4 has an N-terminal L-alanoyl-D-glutamate endopeptidase domain as a catalytic domain and a C-terminal SH3_5 domain as a putative CBD (Fig. 1A). To confirm the cell binding capacity of the SH3_5 domain, we produced EGFP-tagged B4_CBD (Val156-Lys262 of LysB4) and tested its ability to bind diverse species of bacteria (Fig. 1B, Fig. S1). Interestingly, compared to the wide lytic range of LysB4, its CBD specifically binds to *B. cereus* strains (Fig. 1C, Table S3), suggesting that B4_CBD recognizes and binds to conserved cell
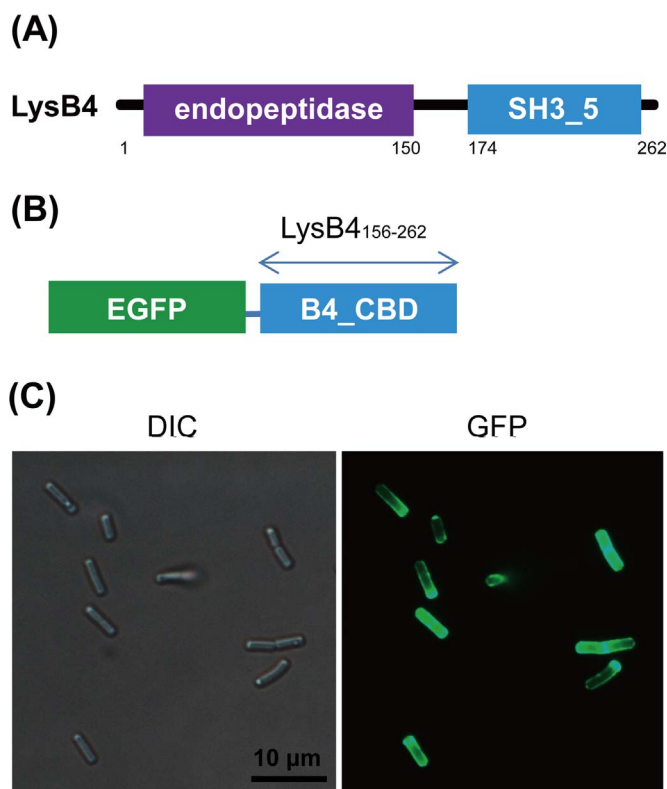

Fig. 1. Identification of the *B. cereus*-specific CBD (B4_CBD) from the endolysin LysB4. (A) Modular structure of LysB4. (B) Schematic representation of the EGFP-tagged B4_CBD. (C) Confirmation of the binding activity of EGFP-B4_CBD to *B. cereus* cells (left, differential interference contrast image; right, GFP fluorescence image).

wall components of *B. cereus*. In addition, B4_CBD showed reasonable binding activities under diverse pH and NaCl conditions (Fig. S2). To test the potential of B4_CBD as an efficient detection probe for *B. cereus*, we performed all further assays in PBS at physiological pH and osmolarity (pH 7.4, 137 mM NaCl, 2.7 mM KCl).

3.2. Establishment of a CBD-based lateral flow assay

Scheme 1 is a schematic illustration of an engineered CBD-based lateral-flow detection system. This system contains two different types of engineered B4_CBDs: Cys-GST-CBD-conjugated AuNPs, which function as detection agents, and MBP-CBDs, which function as capture agents. There are several reasons for the use of the Cys-GST tag as the detection moiety. First, the Cys-GST tag allows simple conjugation of CBD proteins to the AuNP surface because the sulfur of the thiol group (-SH) in the cysteine forms a covalent bond with the gold atom (Xue et al., 2014). In addition, since B4_CBD lacks internal cysteine residues, the addition of a single cysteine residue to the N-terminus enables oriented immobilization, thus preserving the functionality of the immobilized CBDs. The uncovered surface of the gold nanoparticles was blocked by treatment with thiol-functionalized PEG. The GST moiety of the Cys-GST tag enabled the use of commercially available anti-GST antibodies for the control line. The GST also served as a spacer between the CBDs and AuNPs, thereby allowing the CBDs full access to the target cells. Lastly, the GST tag has a stabilizing effect on its fusion partners (Costa et al., 2014), minimizing possible degradation of the CBDs during conjugation and storage.

For capture agents dispensed onto the NC membrane, we initially used B4_CBD, which has no additional tags except a hexa-histidine tag for purification. However, B4_CBD alone was not a satisfactory capture agent because the LOD was found to be 10^6 CFU/mL (Fig. S3). One possibility for the poor performance of B4_CBD as a capture agent is that several residues necessary for cell binding may have been masked or buried by the membrane matrix. Alternatively, the preloaded CBD might have suffered loss of activity during drying. To improve the sensitivity of the assay, we genetically fused MBP to the capture CBD. Our rationale was that MBP is a relatively large (367 amino acids) tag that stabilizes its fusion partner (Costa et al., 2014). Since protein immobilization onto the NC membrane depends on van der Waals forces and electrostatic interactions between the protein and membrane (Kim and Herr, 2013), we hypothesized that the bulky MBP tag, which contains six times more hydrophobic and hydrophilic residues than the CBD, may interface with and immobilize on the membrane more efficiently. If our hypothesis is true, MBP could act as a spacer between the CBD and membrane, reducing steric hindrance so that the binding sites of CBD are more likely to be available to capture target bacteria. Furthermore, the MBP fusion tag enhanced the solubility of the recombinant protein (186 mg of MBP-CBD/L), yielding twice as much protein when expressed in *E. coli* compared to CBD alone (Fig. S1).

3.3. Comparison of antibody and engineered CBDs

To observe whether the genetically fused MBP tag improves the detection sensitivity, the detection results obtained using CBD alone, MBP-CBD, and the commercially available antibody were compared. To the best of our knowledge, the antibody used in this study is the only commercial antibody available that targets *B. cereus*. Fig. 2A and B show that MBP-CBD yielded a stronger detection signal than both CBD alone and the commercial antibody, while no nonspecific reactions were observed in any of the assays. Quantification of the signal intensities (Fig. 2C) also showed that the intensity of the detection signal obtained using MBP-CBD was significantly stronger than that obtained with CBD alone. This result confirms our hypothesis that genetically fusing MBP to the CBD capture agent results in better sensitivity. One possible explanation for this finding is that the MBP tag
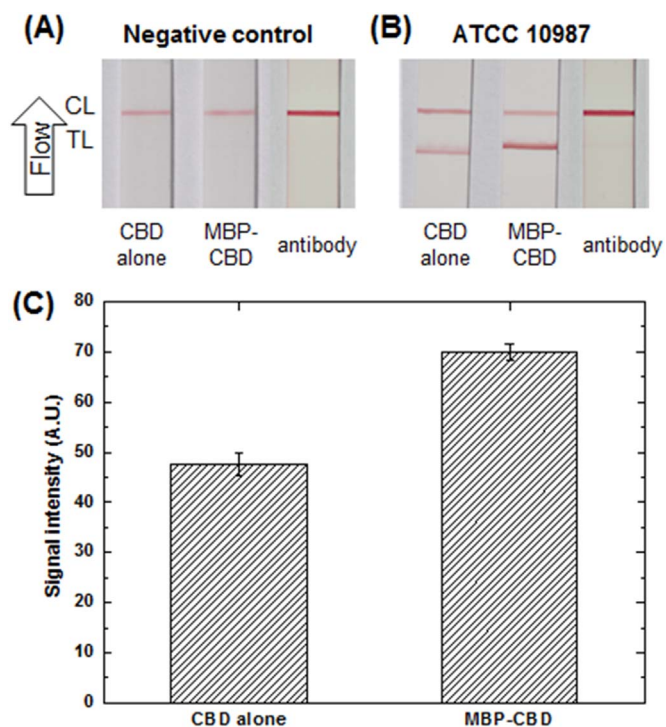

Fig. 2. Assay performance using CBD, MBP-CBD, or the commercial antibody to detect (A) the negative control and (B) 10^7 CFU/mL *B. cereus* (ATCC 10987) (CL: control line, TL: test line). (C) Graph showing that the test line intensity is stronger when using MBP-CBD as a capture molecule compared to CBD alone [(tested with 5×10^6 CFU/mL *B. cereus* (ATCC 10987)].
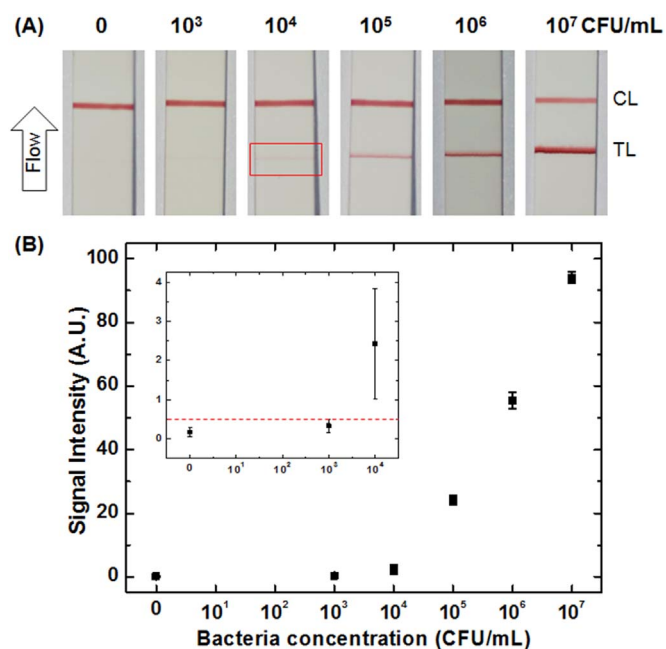

Fig. 3. Detection sensitivity using MBP-CBD. (A) Image showing the detection results of varying concentrations of *B. cereus* (CL: control line, TL: test line). The detection signal starts to appear at 10^4 CFU/mL (indicated by the red box). (B) Quantified signal intensity versus bacteria concentration. The dotted red line in the inset indicates the limit of detection (LOD) (For interpretation of the references to color in this figure legend, the reader is referred to the web version of this article.).

enabled the binding sites of CBD to be more available for capture, thus allowing better binding to the bacteria. It is worth noting that the detection signals were consistent among several different strains of *B. cereus*, indicating robust performance of the engineered CBD (Fig. S4).
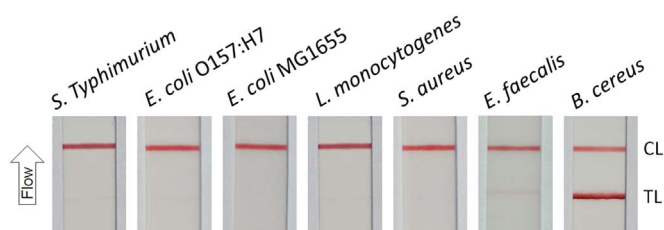
Fig. 4. MBP-CBD specificity. The detection results obtained using strains from different bacterial genera show that CBD is highly specific to *B. cereus* and shows little to no cross-reactivity with other genera (CL: control line, TL: test line).

3.4. Sensitivity

The limit of *B. cereus* detection using MBP-CBD was determined using the ATCC 10987 strain. Since it is important to optimize the concentration of the capture CBD before determining the LOD, the effect of MBP-CBD concentration on signal intensity was first investigated; the optimal concentration was determined to be 3.0 mg/mL (Fig. S5). Fig. 3A shows that the intensity of the test line is proportional to the concentration of the bacteria and that the test line starts to appear at 10^4 CFU/mL (indicated by the red box). It is interesting to note that the control line for 10^7 CFU/mL had a lower intensity than those for lower bacteria concentrations. A likely explanation is that the majority of the CBD-AuNPs are bound to the captured bacteria at the test line, indicating that fewer gold nanoparticles were available to flow past the test line, thereby resulting in a reduced control line intensity. Quantification of the signal intensities (Fig. 3B) showed that the LOD was 10^4 CFU/mL and that the intensity increased with increasing bacteria concentration.

3.5. Specificity

The specificity of MBP-CBD was tested by dipping the test strip into solutions containing 10^7 CFU/mL of bacteria of different genera. Three gram-negative bacteria (*S. typhimurium*, *E. coli* O157:H7, *E. coli* MG1655) and three gram-positive bacteria (*L. monocytogenes*, *S. aureus*, *E. faecalis*) were tested; their detection results were compared to those of *B. cereus* (positive control). As shown in Fig. 4, none of the tested bacteria except for *E. faecalis* showed a detection signal, indicating high specificity of the engineered MBP-CBD. Although MBP-CBD showed slight cross reactivity with *E. faecalis*, this non-specific test signal can be eliminated by minor optimization of the experimental conditions, such as reducing the capture CBD concentration.

4. Conclusions

The present study demonstrates the potential of engineered CBDs in lateral flow-based bacterial detection. Our assay showed better results than traditional antibody-based methods, enabling us to detect as low as 10^4 CFU/mL of *B. cereus* cells within 20 min. Because the CBDs could be produced in large quantities by the *E. coli* expression system, the cost of the assay can be largely reduced. Furthermore, with the increasing number of phage genomes available, this approach could be applied to detect other bacteria using different bacterium-specific CBDs.

Appendix A. Supporting information

Supplementary data associated with this article can be found in the online version at doi:10.1016/j.bios.2017.05.010.

References

Baker, M., 2015. Nature 521, 274–276.
Bottone, E.J., 2010. Clin. Microbiol. Rev. 23, 382–398.
Bruno, J.G., 2014. Pathogens 3, 341–355.
Chen, A., Yang, S., 2015. Biosens. Bioelectron. 71, 230–242.
Costa, S., Almeida, A., Castro, A., Domingues, L., 2014. Front. Microbiol. 5, 63.
Doherty, G.P., Bailey, K., Lewis, P.J., 2010. BMC Res. Notes 3, 303.
Frenzel, A., Hust, M., Schirrmann, T., 2013. Front. Immunol. 4, 217.
Kim, D., Herr, A.E., 2013. Biomicrofluidics 7, 41501.
Kong, M., Ryu, S., 2016. J. Microbiol. Biotechnol. 26, 38–43.
Kong, M., Sim, J., Kang, T., Nguyen, H.H., Park, H.K., Chung, B.H., Ryu, S., 2015. Eur. Biophys. J. 44, 437–446.
Loessner, M.J., Kramer, K., Ebel, F., Scherer, S., 2002. Mol. Microbiol. 44, 335–349.
Posthuma-Trumpie, G.A., Korf, J., van Amerongen, A., 2009. Anal. Bioanal. Chem. 393, 569–582.
Preechakasedkit, P., Pinwattana, K., Dungchai, W., Siangproh, W., Chaicumpa, W., Tongtawe, P., Chailapakul, O., 2012. Biosens. Bioelectron. 31, 562–566.
Robinson, M.P., Ke, N., Lobstein, J., Peterson, C., Szkodny, A., Mansell, T.J., Tuckey, C., Riggs, P.D., Colussi, P.A., Noren, C.J., Taron, C.H., DeLisa, M.P., Berkmen, M., 2015. Nat. Commun. 6, 8072.
Schmelcher, M., Donovan, D.M., Loessner, M.J., 2012. Future Microbiol. 7, 1147–1171.
Sheffield, P., Garrard, S., Derewenda, Z., 1999. Protein Expr. Purif. 15, 34–39.
Smiley, S., Derosa, M., Blais, B., 2013. J. Nucleic Acids 2013, 936542.
Son, B., Yun, J., Lim, J.A., Shin, H., Heu, S., Ryu, S., 2012. BMC Microbiol. 12, 33.
Spadiut, O., Capone, S., Krainer, F., Glieder, A., Herwig, C., 2014. Trends Biotechnol. 32, 54–60.
Tolba, M., Ahmed, M.U., Tlili, C., Eichenseher, F., Loessner, M.J., Zourob, M., 2012. Analyst 137, 5749–5756.
Walcher, G., Stessl, B., Wagner, M., Eichenseher, F., Loessner, M.J., Hein, I., 2010. Foodborne Pathog. Dis. 7, 1019–1024.
Wang, D.B., Tian, B., Zhang, Z.P., Wang, X.Y., Fleming, J., Bi, L.J., Yang, R.F., Zhang, X.E., 2015. Biosens. Bioelectron. 67, 608–614.
Xue, Y., Li, X., Li, H., Zhang, W., 2014. Nat. Commun. 5, 4348.
Yu, J., Zhang, Y., Zhang, Y., Li, H., Yang, H., Wei, H., 2016. Biosens. Bioelectron. 77, 366–371.